Talanta 127 (2014) 100–107

Contents lists available at ScienceDirect

Talanta

journal homepage: www.elsevier.com/locate/talanta

Improved selectivity towards NO_2 of phthalocyanine-based chemosensors by means of original indigo/nanocarbons hybrid material

J. Brunet [a,b,f,*], A. Pauly [a,b,f], M. Dubois [c,d,f], M.L. Rodriguez-Mendez [e,f], A.L. Ndiaye [a,b,f], C. Varenne [a,b,f], K. Guérin [c,d,f]

[a] Clermont Université, Université Blaise Pascal, Institut Pascal, BP 10448, F-63000 Clermont-Ferrand, France
[b] CNRS, UMR 6602, Institut Pascal, F-63171 Aubière, France
[c] Clermont Université, Université Blaise Pascal, Institut de Chimie de Clermont-Ferrand, BP 10448, F-63000 Clermont-Ferrand, France
[d] CNRS, UMR 6002, Institut de Chimie de Clermont-Ferrand, F-63177 Aubière, France
[e] Department of Inorganic Chemistry, Industrial Engineers School, Universidad de Valladolid, P del Cauce 53, 47011 Valladolid, Spain
[f] Laboratoire d'Excellence Mobilité Innovante IMobS3, Université Blaise Pascal, 24 Avenue des Landais, BP 80026, 63171 Aubière Cedex, France

ARTICLE INFO

Article history:
Received 11 December 2013
Received in revised form
21 March 2014
Accepted 27 March 2014
Available online 4 April 2014

Keywords:
Indigo
Nanocarbons
Phthalocyanine
Chemoresistor
Nitrogen dioxide
Sensor selectivity

ABSTRACT

A new and original gas sensor-system dedicated to the selective monitoring of nitrogen dioxide in air and in the presence of ozone, has been successfully achieved. Because of its high sensitivity and its partial selectivity towards oxidizing pollutants (nitrogen dioxide and ozone), copper phthalocyanine-based chemoresistors are relevant. The selectivity towards nitrogen dioxide results from the implementation of a high efficient and selective ozone filter upstream the sensing device. Thus, a powdered indigo/nanocarbons hybrid material has been developed and investigated for such an application. If nanocarbonaceous material acts as a highly permeable matrix with a high specific surface area, immobilized indigo nanoparticles are involved into an ozonolysis reaction with ozone leading to the selective removal of this analytes from air sample. The filtering yields towards each gas have been experimentally quantified and establish the complete removal of ozone while having the concentration of nitrogen dioxide unchanged. Long-term gas exposures reveal the higher durability of hybrid material as compared to nanocarbons and indigo separately. Synthesis, characterizations by many complementary techniques and tests of hybrid filters are detailed. Results on sensor-system including CuPc-based chemoresistors and indigo/carbon nanotubes hybrid material as in-line filter are illustrated. Sensing performances will be especially discussed.

1. Introduction

Amongst all pollutants present into the troposphere, nitrogen dioxide, NO_2 remains a pollutant which requires a special monitoring in view of its dangerousness for health and environment. Its health hazards are well-established: above 80 ppb, respiratory troubles begin to be acute [1]. The US Environmental Protection Agency (EPA) has set the primary standards providing public health protection to 100 ppb for one hour of exposure in ambient air [2]. Coming mainly from vehicle exhaust and combustion processes, its concentration remains still increasing with traffic and building development. In urban atmosphere, NO_2 is the reaction product of nitrogen monoxide (NO) oxidation process with oxygen according to the reaction (1), the kinetics of reaction being fast because of the chemical instability of NO in air.

$$NO + ½\ O_2 \rightarrow NO_2 \quad (1)$$

Since the toxicity threshold of NO_2 is in the concentration range commonly measured in urban and highway environments, its real-time monitoring is a duty for most of the European Union countries. More especially in France, the law on air and the rational use of energy (LAURE law) define the regulatory framework of the monitoring, prevention and forecasting of the air quality as well as public information [3].

To perform the continuous monitoring of pollutants in troposphere, national agencies of air quality control implement local measurement stations throughout the country. Based on

* Corresponding author at: Clermont Université, Université Blaise Pascal, Institut Pascal, BP 10448, F-63000 Clermont-Ferrand, France. Tel.: +33 473 407247; fax: +33 473 407340.
E-mail address: brunet@univ-bpclermont.fr (J. Brunet).

http://dx.doi.org/10.1016/j.talanta.2014.03.064
0039-9140/

spectroscopic analyses tailored to the target pollutant, the standard devices used for concentration quantification are mainly commercial gas analyzers. Although their specifications fulfill to the metrological requirements (high selectivity, low threshold, good resolution and weak response times), they remain not suitable to high resolution mapping or mobile campaigns of measurements. Without being considered as equivalent methods to reference methods used in air quality control context, chemical gas sensors are very attractive to address those applications which gas analyzers cannot satisfy as mentioned above. Undoubtedly, the development of small-size, cheap, easy-use and efficient gas sensors remains worthy of investigation. Nevertheless, the real challenge remains the selectivity because of the coexistence of other interfering pollutants such as ozone (O_3), carbon monoxide (CO), sulfur dioxide (SO_2) and BTX (Benzene, Toluene, Xylenes) in the gaseous phase.

Amongst all the strategies led to enhance this characteristic, many relevant investigations have been performed on the modulation of catalytic activity of metallic oxide sensing devices by the inclusion or surface-deposition of catalytic nanoparticles like Pt [4–6], Pd [7,8] or Ru [9]. The use of hybrid metallic oxide as sensitive material was also a successful way of development [10]. A second approach consists in the implementation of sensing materials involving specific chemical reaction with target gas [11–13] or the synthesis of molecular key–lock system as Molecularly Imprinted Polymer (MIPs). If fruitful results have been previously reported on BTX detection using MIPs [14], the reversibility is often hardly achieved and the detection, limited to gaseous molecules involving weak interaction energies with the sensing layers. A third strategy for the selective metrology of pollutants consists in the use of chemical filters upstream the sensor achieving the complete removal of interfering species while being inert towards the target gas. In such case, the sensing device must be chosen for its high sensitivity to the target gas as well as for its insensitivity to the reactions products which could come from the removal process. Many materials and filtering structures associated with semiconducting gas sensor have been studied for this purpose. Catalytic filters as oxidative agent of interfering species made of porous oxide [15] or metallic materials [16] and membranes acting as physical filters without catalytic activity such as molecular sieves can be mentioned.

An original sensor-system able to perform the selective monitoring of NO_2 in the context of air quality control is detailed in this manuscript. To benefit from a high sensitivity to the target gas, metallophthalocyanines as sensitive materials associated with a resistive transduction mode were chosen, the electrical conductivity being strongly modulated by the sorption of NO_2 and O_3 molecules. The selectivity towards NO_2 will be achieved by in-line filter allowing the selective removal of O_3 from air sample. A great sensitivity, a low threshold of detection, a high resolution as well as a high selectivity to NO_2 is expected. Recent results [17,18] pointed out the efficiency of indigo layer as ozone filter deposited onto a copper phthalocyanine layer leading to a full-organic sensor highly efficient for the selective detection of NO_2. However, some aspects must be improved:

- The low permeability of the filtering structure which results in an increase in response time of the sensing structure,
- the weak extend of the interacting area between gas and indigo molecules (mainly localized at the surface of indigo layer) which results in a moderate durability of the filtering layer and so, in limited lifetime on the sensor-system.

Therefore, the present work especially reports the elaboration, the characterization and the implementation of a new and original organic/inorganic hybrid material developed as a complete, selective and robust ozone filter. This material was obtained by the immobilization of indigo nanoparticles onto a porous nanocarbonaceous matrix exhibiting a high specific surface area. Improvement provided by such a hybrid material as compared to filtering materials previously investigated (indigo an nanocarbons separately) will be illustrated. Included into a sensor-system with phthalocyanine chemosensors, the possibility to perform real-time monitoring of nitrogen dioxide will be assessed and discussed.

2. Experimental

2.1. Materials

Indigo powder was purchased from PCUK company (Produits Chimiques Ugine Kuhlmann). Mass spectrum (Chemical ionization) showed the presence of only one signal at $m/z=263$ (corresponding to protonated indigo molecule, MH+). Elemental analysis found the following composition C 72.30; H 3.74; N 10.57%, in agreement with theoretical ones C 73.27; H 3.84; N 10.68%, calculated for $C_{16}H_{10}N_2O_2$.

The Multi-Wall-Carbon-NanoTubes were provided by CNano-Technology Limited corporation (*named MWCNTs Cnano*). They were obtained by chemical vapor deposition (CVD) with a purity given higher than 90%.

2.2. Characterizations

Nitrogen adsorption isotherms were measured at 77 K using a Micromeritics ASAP 2020 automatic apparatus. Before measurements, samples were outgassed under secondary vacuum at 300 °C during 2 h for sufficient removal of adsorbed impurities.

Powdered Indigo was investigated by a Thermo Nicolet 5700 FT-IR spectrometer in the range 400–4000 cm^{-1} with 4 cm^{-1} resolution.

TGA experiments were carried out on Shimadzu TGA-50. Measurements are made in air at a heating rate of 2 °C min^{-1} from room temperature to 600 °C on 14.3 mg of sample (accuracy of 0.1 mg).

SEM Micrographs were recorded using a Cambridge Scan 360 SEM operating at 3 kV.

2.3. The filtering test bench

The experimental test bench especially developed to assess the filtering efficiency of all the powdered materials investigated in this study was previously detailed [18]. Powders are confined into a polytetrafluoroethylene (PTFE) gas exposure chamber between two PTFE membranes with low porosity (pore size=5 μm). The filtering yields of each material exposed to well-controlled concentrations of O_3 and NO_2 in synthetic air were extracted from the measurement of gas concentrations upstream and downstream the exposure chamber by means of commercial gas analyzers. The filtering yields were determined in the 20–200 ppb range. Fig. 1 depicts the typical gas concentration evolution in time observed for a material which can be considered as a high-efficient filter because it ensures a complete removal of polluting gas in air sample. For more technical details, please refer to previous paper [18].

3. Results and discussions

3.1. Copper phthalocyanine-based chemoresistor: a first level of selectivity

Most of the semiconductor gas sensors are chemoresistors implementing a thin layer of semiconducting material which

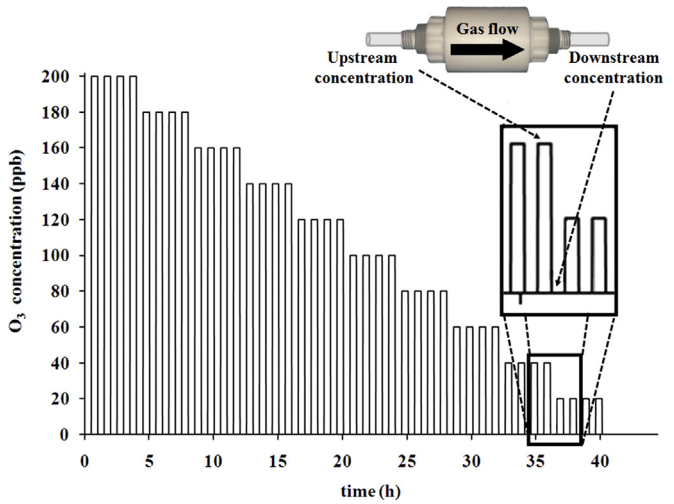

Fig. 1. Filtering yield assessment of powdered materials by consecutive gas concentration measurements upstream then downstream the exposure chamber. Investigated materials were exposed to each concentration from 200 ppb to 20 ppb with 20 ppb as concentration step during 4 h. During each exposure, 4 successive upstream/downstream measurements of concentration were performed. Note that this result is typical from an ideal filter (complete gas removal downstream the cartridge).

interacts with gases [19–21]. The modulation of the doping rate of the semiconductor by adsorbed gaseous species, which injects or traps the free charge carriers of the material close to the surface, results in the variation of its electrical conductivity. Acting as reversible doping elements, the gaseous molecules are responsible of an extrinsic conductivity into the semiconductor in addition to the intrinsic one [22]. Thus, the effect of doping gases on the conductivity is extended if the intrinsic conductivity of the sensing material is low, provided thus a great reactivity to sensing devices.

According to the mechanisms of interaction implicated, the potentially detectable gases with such sensing devices are those able to involve reversible oxidizing or reducing reactions with the material. In accordance with the electrochemical model formalizing the interactions between gases and MPc layers [23], all experimental results demonstrate that neutral organic materials, like non-radical and unsubstituted planar phthalocyanines, are very sensitive to strong oxidizing gases like O_3, NO_2 and Cl_2 (their Electron Affinities EA are respectively 2.10 eV, 2.20 eV and 2.35 eV [24,25]) and rather insensitive to reducing ones like NH_3 or CO. Such sensitivity to oxidizing gases is responsible for their electronic nature. Indeed, taking into consideration the value of the band gap (close to 2 eV) and their very low intrinsic conductivities at room temperature under vacuum, unsubstituted metallophthalocyanines are intrinsically insulating. Nevertheless, their high chemical affinity with oxidizing gases present in the atmosphere results in a non-intentional doping process by gaseous molecule, leading to an increase in its electronic conductivity (p type). Therefore, these phthalocyanines can be commonly considered like doped insulators instead of semiconductors. The intrinsic conductivity of unsubstituted metallophthalocyanines remains low whereas the extrinsic one strongly increases in the presence of oxidizing analytes. These materials are thus especially attractive for the development of highly sensitive sensors as stated above.

Because our objectives were focused on the development of NO_2 gas sensor-systems, copper phthalocyanine (CuPc) was chosen as a relevant sensitive semiconductor to develop chemosensors. Beyond to benefit from a high sensitivity, such a molecular material provides a first level of selectivity towards oxidizing analytes. Indeed, numerous experimental data related with the detection of oxidizing gases with phthalocyanine layers were reported [26]. Experiments clearly established that the electronic conductivity of a CuPc thin layer strongly increases with NO_2 and O_3 exposure even in sub-ppm concentration range [27–30]. In the same experimental conditions, O_2 has a small effect even if this gas is present at 20%. Amongst all the pollutants simultaneously present in low atmosphere, only NO_2 and O_3 induce significant electrical responses on CuPc chemoresistors. A partial selectivity is thus achieved. O_3 being the most interfering pollutant to perform a complete selectivity towards NO_2, we suggest to develop in-line or integrated filter completely impervious to O_3 while being inert towards NO_2.

3.2. Potentialities of indigo as ozone filter

Morphological and structural characterizations have been made on powdered indigo samples. The FTIR experimental spectrum of indigo powder has been firstly compared to the standard IR spectrum of indigo given by the National Institute of Standards and Technology (NIST) to attest of the chemical nature of our material. Although a strong spectral contamination due to oil around 2900 cm^{-1} appears on NIST data [31], the two spectra are closely similar in all the wavenumber range investigated. Our commercial indigo powder corresponds to synthetic indigo and not to one of its derivatives (e.g., indigo carmine). The morphology of indigo powder was determined by scanning electron microscopy, micrograph being reported in Fig. 2a. The picture underlines a high divided state with a lamellar structure. Indigo grains are constituted by an agglomeration of micrometric-sized flakes.

The specific surface area (SSA) corresponding to the surface area available for gas adsorption and the nature of the porosity were deduced from nitrogen adsorption/desorption isotherm at 77 K. The profile of the isotherm experimentally determined for indigo powder (not given here) was compared to those given as reference in the classification established by the International Union of Pure and Applied Chemistry (IUPAC) [32]. It is a type II isotherm which corresponds to a non-porous or macroporous adsorbent. Moreover, a slight hysteresis typical from multilayer adsorption was observed. By comparison with IUPAC classification, the hysteresis loop without any limit of adsorption at high partial pressure corresponds to type H3 loop which is significant of aggregates of plate-like particles. Results from N_2 adsorption at 77 K corroborates the flake structure of indigo sample observed on SEM pictures. The porosity of indigo is mainly inter-granular rather than intra-granular. The specific surface area extracted from BET isotherm was assessed to 15.2 $m^2\ g^{-1}$.

Once characterized, the behavior of indigo powder towards NO_2 and O_3 exposures has been studied. More especially, its filtering efficiency, its potential filtering selectivity and its durability were quantified. With this objective, two classes of measurement have been made:

- Cyclic measurements of gas concentrations upstream then downstream the filter exposed to NO_2 and O_3 in the 20–200 ppb range to calculate the filtering yields and estimate the level of selectivity;
- cyclic measurements of gas concentrations upstream then downstream the filter continuously exposed to 850 ppb of O_3 to evaluate the durability and the lifetime of the material versus cumulated gas concentration. The filtering yield η was calculated from upstream and downstream concentrations, respectively C_{up} and C_{down}, according to the relation 2

$$\eta(\%) = 100 \times (C_{up} - C_{down})/C_{up} \quad (2)$$

Fig. 3a represents the cyclic measurements of O_3 concentration successively upstream then downstream a cartridge full of indigo

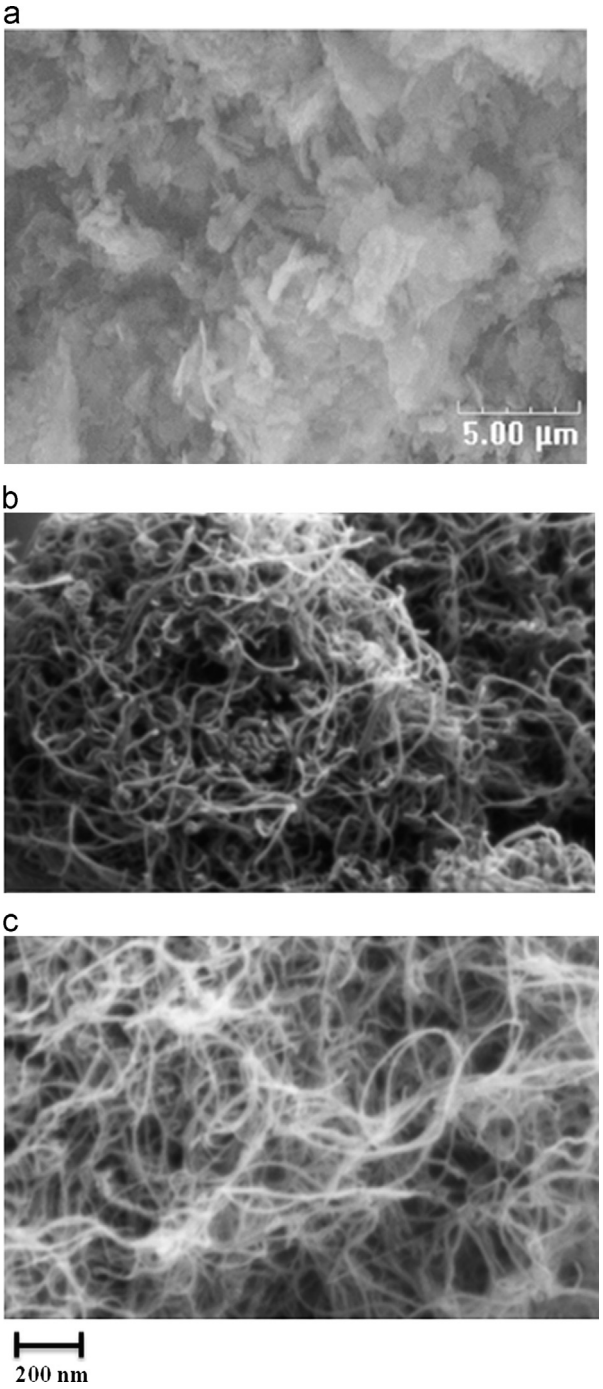

Fig. 2. SEM micrographs of (a) indigo powder with magnification × 5000, (b) untreated MWCNTs, and (c) indigo/MWCNTs hybrid material.

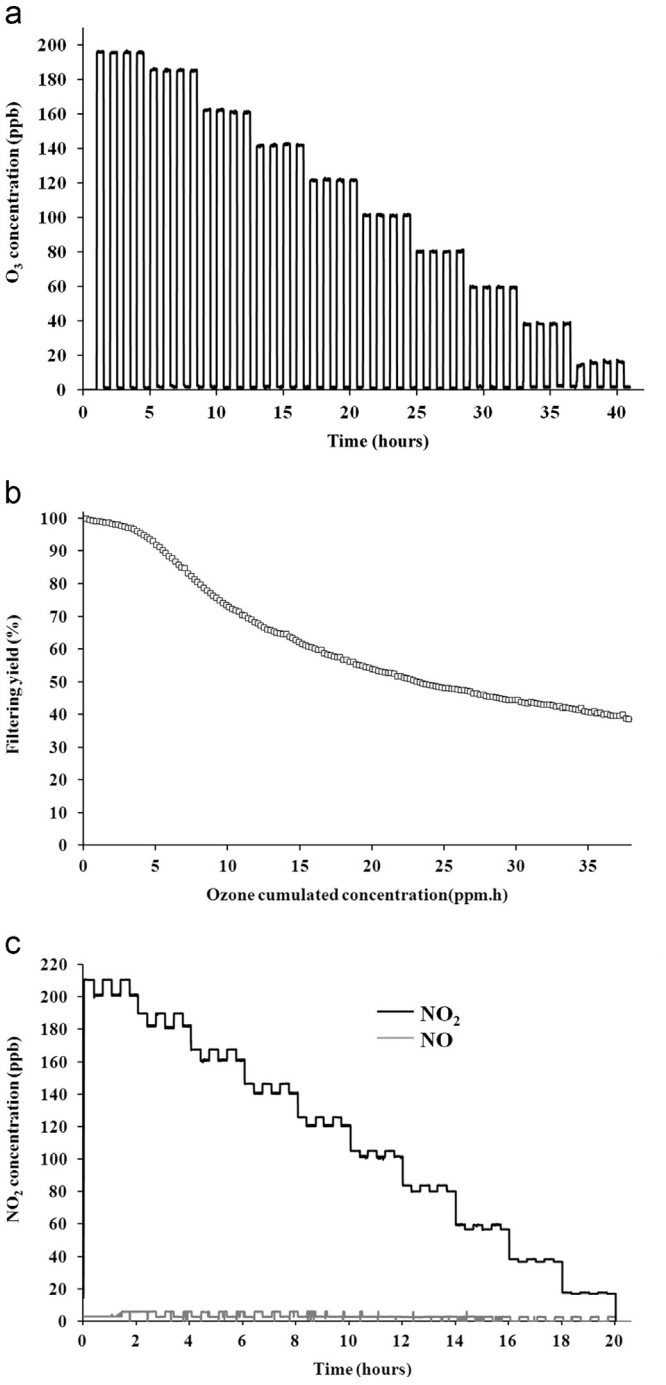

Fig. 3. Filtering performances of indigo powder towards oxidizing gases at room temperature (a) filtering yield measurement towards ozone in the 20–200 ppb concentration range, (b) filtering yield evolution with cumulated O_3 concentration, and (c) nitrogen dioxide and nitrogen monoxide concentrations successively measured upstream then downstream the filter exposed to nitrogen dioxide in the 20–210 ppb range.

powder exposed to gas concentration in the 20–200 ppb range. Results clearly show that indigo exhibits a filtering efficiency towards ozone close to this of an ideal filter as depicted in Fig. 1. More quantitatively, the filtering yield η_{O_3} remains higher than 99% whatever the concentration. In order to estimate the level of filtering selectivity of indigo, similar measurements have been achieved with NO_2. Thus, Fig. 3c represents experimental results obtained towards NO_2 in the same experimental conditions as for O_3 investigations. The reactivity between NO_2 and indigo remains weak and small proportion of NO_2 concentration is removed from polluted air sample. Whatever the concentration, the filtering yield remains lower than 4% and no significant NO production can be noticed. As a consequence, indigo can be considered as a high-efficient and selective O_3 filter in our experimental conditions. To estimate the durability of indigo powder under O_3 exposure, the filtering yield has been continuously monitored during a long exposure of the material to 850 ppb of O_3. Fig. 3b represents the evolution of the filtering yield as a function of the cumulated ozone concentration in ppm · h. We can observe a continuous decrease in the filtering yield from 100%, corresponding to the result given in Fig. 3a to 40% for a cumulated concentration close to 35 ppm · h. The half life time can be

estimated to 23 ppm · h approximately. In atmospheric conditions, its durability is sufficient to ensure many days of ozone removal. For an average outdoor O_3 concentration close to 25 ppb corresponding the annual average concentration in France in 2012, the filtering yield remains higher than 90% during more than 9 days.

The well-known chemical reaction of ozone on indigo grains corresponds to a chemisorption process which provides two reaction products when reaction occurs in dry conditions: isatin and isatoic anhydride. When reaction takes place under wet conditions, only one product (isatin) is obtained. Such reaction, called ozonolysis and corresponding to an electrophilic addition to the unsaturated C=C bond of indigo was already implemented for ozone titration in aqueous phase [33] as well as in gaseous phase [34,35]. The gradual fading from blue to yellow resulting from the superficial ozonolysis of thin indigo layer has been already exploited for the development of very sensitive ozone sensors [36,37]. To estimate the extend of ozonolysis mechanism on indigo grain, FT-IR analysis on non-exposed powder and on powder exposed to 37.85 ppm · h of O_3 were performed. The spectra are reported in Fig. 4. The comparison between the two IR spectra shows only an additional vibration band which appears at 1732 cm^{-1}. This band can be attributed to the C=O bond in alpha position of N–H bond into the molecule of isatin [38]. Nevertheless, although the filtering yield has strongly decreased consecutively to O_3 exposure in such conditions, the intensity of this C=O vibration band remains weak. This result highlights that ozonolysis reaction affects a weak part of material and remains mainly localized at the surface of indigo grains. Ozone being chemically unstable, its diffusion into the bulk is unlikely. Ozonolysis acts as a passivation process which slowly annihilates the filtering properties of indigo. The weak reaction of NO_2 on indigo as well as the non-significant increase in NO concentration during gas exposure can be attributed to a low energy process like diffusion/physisorption. The low filtering yield measured is interpreted as retention of diffused nitrogen molecules in the volume of indigo particles. If indigo powder is relevant as selective O_3 filter, the main drawback remains its limited durability due to its low specific surface area and to the ozonolysis reaction only entailing the superficial indigo molecular units. To improve this durability, our strategy was to develop indigo filter with high surface-volume ratio. For this purpose, the development of hybrid indigo/nanocarbons material seems attractive to benefit from the high specific surface area of nanocarbonaceous matrix.

3.3. Development of hybrid indigo/nanocarbons filter

3.3.1. Multi-walled nanocarbons as matrix for impregnation

Our strategy is motivated by the ability of indigo molecules to be impregnated on the surface of a highly permeable matrix provided with a high surface of adsorption. Moreover, a thin superficial impregnation of the matrix avoids the passive character of the indigo molecules into the bulk of the powdered material. Thus, the whole surface of the filter will be easily reached by gas and a diffusion process will not be necessary to access to chemically active sites. A durability enhancement is so expected. The first key point concerns the choice of the permeable matrix for the immobilization of indigo particles.

The carbonaceous materials, such as activated carbons [39], graphite [40], carbon nanotubes (single and multi walled, SWCNTs and MWCNTs, respectively) [41] or carbon nanofibers (CNFs) [42] have been fruitfully implemented as functional elements in gas sensors [43,44] and membranes [45]. The nanostructured carbonaceous compounds constitute a panel of material with specific physical and chemical properties. The morphology, the stacking modes as well as the various arrangements of graphene sheets are responsible of such diversity and give access to various and numerous applications. The potentialities of some nanocarbons to be used as selective chemical filter towards oxidizing gases have been previously demonstrated. In particular, we have established the complete ozone removal by all the investigated nanocarbons [46,47]. The physical and chemical mechanisms involved between nanocarbons and ozone corresponding to oxidation and their influences on the electrical conductivity of SWCNTs have been already characterized by Raman spectroscopy, XPS and UPS [48]. The increase in the structural defects on the sidewalls of the nanotubes consecutively to O_3 exposure, the irreversible formation of oxidized carbon species (mainly ethers, epoxides and carbonyls groups) and the removal of the aromatic character of nanotubes have thus been established. These results are in total agreement with our previous works and highlight the relevance of nanocarbons as materials for ozone removal [47]. The kinetics of oxidation at room temperature being fast [48], the removal is immediate. Moreover, the high specific surface area of the material and the great number of chemisorption sites (aromatic ring, dangling bonds) are responsible for the durability of the material and so, the filter lifetime.

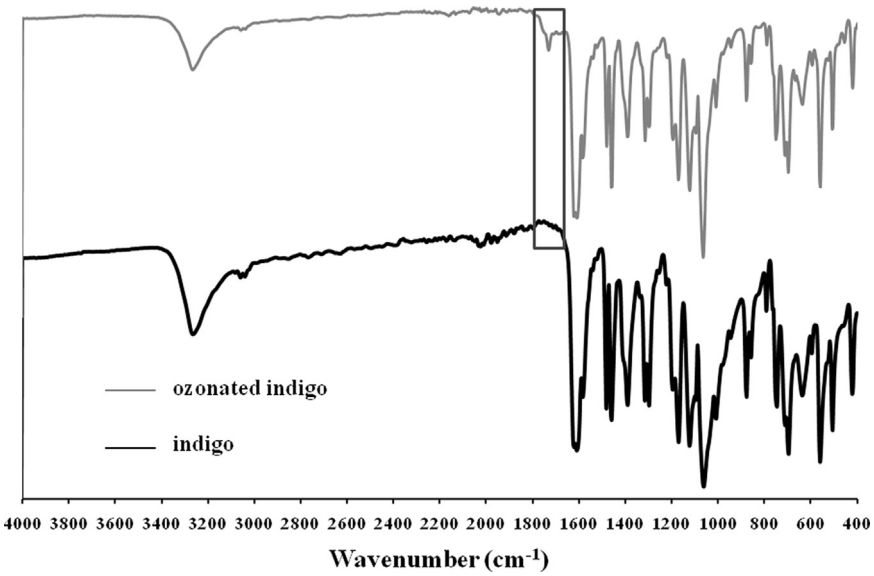

Fig. 4. IR spectra of unexposed indigo powder and continuously exposed to 850 ppb of ozone during 60 h.

Because the immobilization of indigo particles could correspond to a partial functionalization of the carbonaceous matrix (not complete impregnation), selected nanocarbons must exhibit the most important specific surface area while being inert towards the pollutant we aim to detect, NO_2. Amongst all the investigated nanocarbonaceous materials and taking into consideration the specifications previously describe, multi-walled carbon nanotubes from CNanoTechnology Limited Corporation (MWCNTs Cnano) are the most judicious. Such material exhibits a 182 $m^2 g^{-1}$ SSA, an O_3 filtering yield close to 97% and a filtering yield towards NO_2 less than 3%. These data point out the capacity of MWCNTs Cnano to be a well-adapted matrix reaching conciliation between its chemical inertia toward NO_2, the value of its total surface of adsorption and great potentialities for indigo immobilization.

3.3.2. *Elaboration of indigo impregnated filtering structures*

Our synthesis is based on the maximal solvatation of indigo molecules in an efficient solvent. A preliminary study was then performed to target the best solvent for indigo dispersion among the following four organic solvents: dimethylsulfoxide (DMSO), methanol, acetone and acetonitrile. For each solvent, a saturated solution was prepared by successive additions of indigo and the saturation concentration was determined as summarized in Table 1. The analysis of the physical properties of the different solvents reveals that acetonitrile is the most suitable for our application. Indeed, in spite of a saturation concentration (SC) more important in DMSO (70 mg l^{-1}), the evaporation temperature of this solvent is high (189 °C) and may result in chemical changes on indigo molecules. Methanol was avoided because it exhibits the lowest SC, with only 12 mg l^{-1}. Acetone, with SC of 50 mg l^{-1}, appears as an appropriate solvent. However, the UV–visible absorbance measured with increasing concentrations of indigo provides a calibration curve which is not in agreement with the Beer–Lambert's law. Finally, in the case of acetonitrile, the calibration respects the Beer–Lambert's law and thanks to an evaporation temperature of 81.6 °C, the elimination of the solvent will result in any change neither on the carbon structure nor on the organic molecule. The maximal concentration of indigo in acetonitrile was assessed to 30 mg l^{-1}.

This concentration remaining low, the impregnation has been made by several additions of saturated solution on MWCNTs to obtain the highest amount of adsorbed indigo on the carbonaceous surface. Impregnation process has been monitored by means of UV–vis spectroscopy on the indigo solution at the maximum of absorbance, i.e., 600 nm in our experimental conditions. The protocol used for the functionalization of carbons nanotubes by indigo can be summarized as follow:

- 2 mg of MWCNTs in contact with 4 ml of saturated indigo solution then sonication,
- analysis of supernatant liquid phase by UV–vis spectroscopy after decantation,
- determination of absorbance at 600 nm,
- if absorbance was close to 0 (indigo completely adsorbed onto nanocarbons), 2 ml of indigo solution was added, this step being replicated until saturation,
- if absorbance was different from 0, amount of indigo immobilized on carbonaceous matrix was deduced from the absorbance of supernatant liquid and the reference solution (solution saturated with indigo).

Table 1
Maximum indigo concentrations in DMSO, methanol, acetone and acetonitrile saturated solutions.

Solvents	DMSO	Methanol	Acetone	Acetonitrile
Saturation concentration (mg l^{-1})	70	12	50	30

According to this protocol, the mass ratio of indigo immobilized on carbon nanotubes in saturation conditions was assessed to 144 mg per gram of MWCNTs.

The functionalization of nanocarbons by indigo was then revealed by complementary techniques of analysis: Scanning Electron Microscopy (SEM) and ThemoGravimetric Analysis (TGA). SEM micrographs of untreated (a) and functionalized (b) carbon nanotubes are given in Fig. 2b and c. A cotton-like aspect due to the electrical insulting property of indigo can be noticed and so highlights its adsorption on MWCNTs. Such conclusions are strengthened by TGA thermograms reported in Fig. 5. Two mass losses can be observed:

- A first occurring at 340 °C and corresponding to indigo sublimation, the sublimation temperature of our indigo sample having been measured close to 280 °C in air,
- a second occurring between 400 and 600 °C which can be attributed to carbon decomposition.

From the weight loss, the proportion of indigo immobilized on MWCNTs was estimated to 200 mg per gram of carbon, in relative good accordance with the amount obtained from UV–visible spectroscopy (144 mg/g of C). The results from TGA and picture from SEM unambiguously attest of the presence of indigo on MWCNTs. Taking into consideration the presence of benzene rings on both indigo and nanocarbons as well as the low increase in sublimation temperature of indigo for hybrid material, we interpret that the adsorption process should involve pi-stacking interactions. So, the impregnation could be considered as a non-covalent functionalization of nanocarbonaceous matrix.

3.3.3. *Filtering properties*

Once prepared and characterized, the filtering yields and the durability of indigo/MWCNTs hybrid material towards the target gases NO_2 and O_3 were experimentally determined. The experimental protocols for gas exposures were the same as those relative to indigo previously detailed in Section 3.2. While the filtering yield towards ozone was higher than 99% for only indigo, it reaches 99.5% for indigo/MWCNTs. For nitrogen dioxide, 4.0% have been measured for the filtering yield for indigo against now 3.6% for indigo/MWCNTs. If these values remain closely similar, a slight increase in selectivity towards O_3 is noticeable. In contrast, the most significant enhancement has been obtained on the filter durability. Supporting evidence,

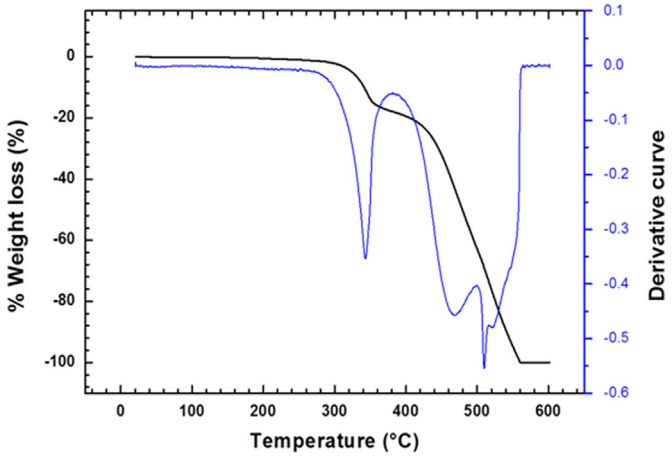

Fig. 5. Thermograms and its derivative curve of indigo/MWCNTs hybrid material.

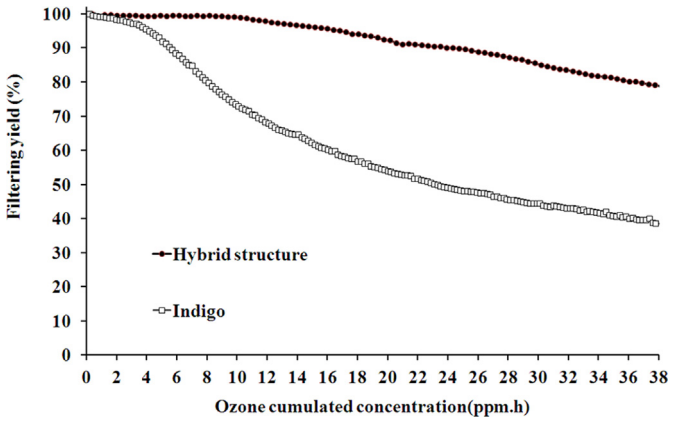

Fig. 6. Comparative evolution of the filtering yields of indigo powder and indigo/MWCNTs as a function of cumulated ozone concentration (in ppm · h).

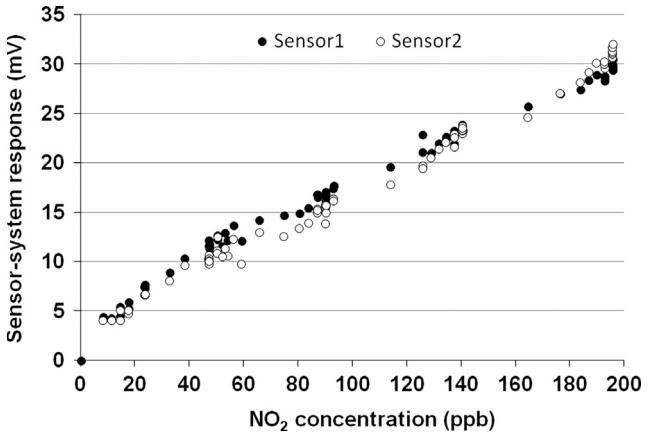

Fig. 7. Calibration curves of sensor-system implementing two phthalocyanine-based chemoresistors towards nitrogen dioxide in the 10–200 ppb range. The sensing structures as well as their working conditions are perfectly similar.

Fig. 6 depicts the comparison of the time-dependence of the filtering yield of the indigo powder and the hybrid material continuously exposed to 850 ppb of O_3. A slow and continuous decrease in the filtering efficiency which corresponds to the irreversible ozonolysis of indigo thin layer is manifest. However, we can notice that the filter lifetime is strongly improved by the impregnation process. If we consider a loss of 10% of the O_3 filtering yield from its maximum, this corresponds to an exposure to 5.5 ppm · h for powdered indigo and 24.2 ppm · h for immobilized indigo. As expected above, such a result can be justified by the higher effective surface of adsorption and so, is a consequence of the increase in surface/volume ratio of the layer.

3.4. Development of sensor-system dedicated to NO_2 monitoring

The sensor-system developed in this work combines two strategies. On one hand, it takes advantage of the partial selectivity of phthalocyanine-based chemoresistors to strong oxidizing analytes (NO_2 and O_3). On the other hand, it profits from the selective and sustainable O_3 removal by indigo/MWCNTs hybrid filters. Thus, the chemoresistors consist in thin films of 300 nm copper phthalocyanine (CuPc) prepared by physical vapor deposition (PVD) under vacuum on an alumina substrate (3×5 mm^2) fitted with interdigitated Pt electrodes (IDEs) to monitor the electrical conductivity of the sensitive layer [49]. A methodology of measurements which exploits the kinetics of sensor response previously developed with such sensing structures is applied. It overcomes the problem of the long response time these sensors suffer and improves the reproducibility of measurements by reducing drifts in sensor responses. To summarize, this methodology consists in two sequences:

- Sensing layer is exposed to pollutants through the indigo/MWCNTs hybrid filter during short time (2 min) and at low temperature, the sensor-system response being defined as the differential conductivity during this step,
- sensing layer is then regenerated under clean air through an integral filter (charcoal) at higher temperature to ensure a complete desorption of adsorbed gaseous species.

The sampling time was chosen in accordance with the specifications of the French Network of Air Quality Control and the sensor-system delivers one measurement each 15 min. All experimental details were previously described in a dedicated publication [50]. To benefit from a signal which can be easily stored in an electronic memory, a conductivity/voltage conversion is implemented close to the sensor. Thus, sensor-system response is a voltage image of the variation of electrical conductivity during pollutant exposures. This variation is due the creation of extrinsic p-type charge carriers in the sensitive material by charge transfer between the adsorbed oxidizing gaseous molecules and the phthalocyanine molecular units [51].

The calibration curve of a sensor-system implementing two phthalocyanine-based chemoresistors located downstream of an in-line hybrid filter has been finally performed. Fig. 7 represents the sensor-system responses versus nitrogen dioxide concentrations in the 10–200 ppb range for the two similar sensing structures with the same working conditions. NO_2 concentrations were continuously monitored by a chemiluminescent commercial NO_X analyzer (model 42i, ThermoElectron Corporation) located downstream our gas sensor-system. Let us remind that the sampling time was set to 15 min. Results highlight a threshold of detection close to few ppb, a low dispersion of measurements, a resolution higher than 10 ppb and a linear response in the 20–200 ppb concentration range. Moreover, taking into consideration the slow kinetics of pollutant concentration variations in outdoor environments, a real-time monitoring of NO_2 in the context of air quality control can be successfully achieved. A good reproducibility can be also underlined as justified by the close responses and the similar behavior towards NO_2 obtained for the two sensors. Similar measurements have been made with ozone in the same concentration range thanks to UV photometry commercial O_3 analyzer (model 49i, ThermoElectron Corporation). Although data are not reported in Fig. 7, no significant response was obtained for ozone, sensor signal not being distinguished from the electronic noise. A high level of selectivity is performed. In our working conditions and for an average ozone background level to 50 ppb, the sensor-system lifetime mainly conditioned by the efficiency of indigo/MWCNTs hybrid filter to remove this interfering pollutant was estimated to more than 3 months. Although this hybrid filter is especially appropriate in such sensor-system, it could be associated to others chemical sensors for which ozone represents the major interfering gas.

4. Conclusion

The present study deals with a sensor-system achieving the selective monitoring of nitrogen dioxide in an environmental context. The sensing element is based on a copper phthalocyanine-based chemoresistor which exhibits a partial selectivity to strong oxidizing species in air, i.e., ozone and nitrogen dioxide. The selectivity towards nitrogen dioxide was successfully performed by the implementation of an in-line chemical filter obtained by the immobilization of indigo

particles on nanocarbonaceous matrix. The protocol of synthesis has been optimized in regards on the solvent used and is detailed. SEM micrographs as well as thermogravimetric analysis bring out this non-covalent functionalization. Filtering yield measurements towards NO_2 and O_3 highlight its efficient and selective removal of O_3 from air sample. Tests of durability by long-term ozone exposures especially underlines its higher filtering lifetime as compared to powdered indigo and nanocarbons considered separately. Results of an original sensor-system prototype strengthen its ability to selectively monitor NO_2 despite the presence of ozone in its environment. A threshold close to few ppb, a resolution higher than 10 ppb and a high level of reproducibility open the way to air quality control applications.

Acknowledgments

This work was funded by grants from the French program "*investissement d'avenir*", the European Commission (Auvergne Feder funds) and the "Région Auvergne" in the framework of the LabEx IMobS^3

Professor Maria-Luz Rodriguez-Mendez, from University of Valladolid (Spain), was invited for 2 months in order to be involved in the project "Selective Chemical Sensors".

A.L. Ndiaye thanks the "Laboratoire d'Excellence IMobS^3" for postdoctoral fellowship.

This work involves some developments associated to the CAPBTX project (2010 BLAN 917 01) and the authors wish to gratefully acknowledge the Agence Nationale de la Recherche (A.N.R., France).

J. Brunet, A. Pauly and A.L. Ndiaye would like to thank the transdisciplinary COST Action TD 1105 "EuNetAir" in which they are involved for supporting these scientific works.

References

[1] International Center for Technology Assessment, In-Car Air Pollution: the Hidden Threat to Automobile Drivers: Report No. 4, An Assessment of the Air Quality inside Automobile Passenger Compartments, July 2000.
[2] P. Koutrakis, J.M. Wolfson, A. Bunyaviroch, S.E. Froehlich, K. Hirano, J.D. Mulik, Anal. Chem. 65 (1993) 209–214.
[3] Act No. 96-1236 of 30 December 1996 on the air and the rational use of energy, Official Journal L220-1, 1 January 1997.
[4] J. Wollenstein, H. Bottner, M. Jaegle, W.J. Becker, E. Wagner, Sens. Actuators B 70 (2000) 196–202.
[5] M. Fleischer, S. Kornely, T. Weh, J. Frank, H. Meixner, Sens. Actuators B 69 (2000) 205–210.
[6] C.O. Park, S.A. Akbar, J. Hwang, Mater. Chem. Phys. 75 (2002) 56–60.
[7] G.G. Mandayo, E. Castano, F.J. Garcia, A. Cirera, A. Cornet, J.R. Morante, Sens. Actuators B 87 (2002) 88–94.
[8] A. Cabot, J. Arbiol, A. Cornet, J.R. Morante, F. Chen, M. Liu, Thin Solid Films 436 (2003) 64–69.
[9] A. Ryzhikov, M. Labeau, A. Gaskov, Sens. Actuators B 109 (2005) 91–96.
[10] M. Nacken, S. Heidenreich, M. Hackel, G. Schaub, Appl. Catal. B Environ. 70 (2007) 370–376.
[11] T. Tanaka, T. Ohyama, Y.Y. Maruo, T. Hayashi, Sens. Actuators B 47 (1998) 65–69.
[12] T. Ohyama, Y.Y. Maruo, T. Tanaka, T. Hayashi, Sens. Actuators B 64 (2000) 142–146.
[13] M.I.H. Helaleh, S. Ngudiwaluyo, T. Korenaga, K. Tanaka, Talanta 58 (2002) 649–659.
[14] M. Matsuguchi, T. Uno, Sens. Actuators B 113 (2006) 94–99.
[15] M. Fleischer, H. Meixner, Sens. Actuators B 52 (1998) 179–187.
[16] P. Dutronc, C. Lucat, F. Ménil, M. Loesch, L. Combes, Sens. Actuators B 15 (1993) 24–31.
[17] J. Brunet, L. Spinelle, A. Pauly, M. Dubois, K. Guerin, M. Bouvet, C. Varenne, B. Lauron, A. Hamwi, Organ. Electron. 11 (2010) 1223–1229.
[18] J. Brunet, L. Spinelle, A. Ndiaye, M. Dubois, G. Monier, C. Varenne, A. Pauly, B. Lauron, K. Guerin, A. Hamwi, Thin Solid Films 520 (2011) 971–977.
[19] R. Zhou, F. Josse, W. Gopel, Z.Z. Ozturk, O. Bekaroglu, Appl. Organomet. Chem. 10 (1996) 557–577.
[20] A. de Saja, M.L. Rodriguez-Mendez, Adv. Colloid Interface 116 (2005) 1–11.
[21] N. Kılınç, D. Atilla, S. Öztürk, A.G. Gürek, Z.Z. Öztürk, V. Ahsen, Thin Solid Films 517 (2009) 6206–6210.
[22] M. Passard, A. Pauly, J.P. Blanc, S. Dogo, J.P. Germain, C. Maleysson, Thin Solid Films (1994) 272–276.
[23] C.A. Grimes, E.C. Dickey, M.V. Pishko, Encyclopedia of Sensors, American Scientific Publishers, Stevenson Ranch, CA, USA, 2006.
[24] R. Weast, S.M. Selby, C.D. Hodgman, Handbook of Chemistry and Physics, 46th ed., The Chemical Rubber Co., Cleveland, 1964–65.
[25] Y.J. Huheey, Inorganic Chemistry: Principles of Structure and Reactivity, Harper and Row, New-York, 1993.
[26] J.D. Wright, Prog. Surf. Sci. 31 (1989) 1–60.
[27] S. Dogo, J.P. Germain, C. Maleysson, A. Pauly, Thin Solid Films 219 (1992) 251–256.
[28] J. Brunet, A. Pauly, L. Mazet, J.P. Germain, M. Bouvet, B. Malezieux, Thin Solid Films 490 (2005) 28–35.
[29] J. Brunet, L. Talazac, V. Battut, A. Pauly, J.P. Blanc, J.P. Germain, S. Pellier, C. Soulier, Thin Solid Films 391 (2001) 308–313.
[30] C. Maleysson, M. Passard, J.-P. Blanc, V. Battut, J.-P. Germain, A. Pauly, V. Demarne, A. Grisel, C. Tiret, R. Planade, Sens. Actuators B 26-27 (1995) 144–149.
[31] Information on ⟨http:/webbook.nist.gov/chemistry/⟩.
[32] K.S.W. Sing, Pure Appl. Chem. 54 (1982) 2201–2218.
[33] K. Takeuchi, T. Ibusuki, Anal. Chem. 61 (1989) 619–623.
[34] M. Alexy, G. Voss, J. Heinze, Anal. Bioanal. Chem. 382 (2005) 1628–1641.
[35] E.P. Felix, K.A.D. De Souza, C.M. Dias, A.A. Cardoso, J. AOAC Int. 89 (2006) 480–485.
[36] J. Li, Q. Li, J.V. Dyke, P.K. Dasgupta, Talanta 74 (2008) 958–964.
[37] Y.Y. Maruo, T. Kunioka, K. Akaoka, J. Nakamura, Sens. Actuators B 135 (2009) 575–580.
[38] C. Pârnău, A. Kriza, N. Popa, S. Udrea, Analele Univ. Bucur. – Chim. Anul XIV I–II (2005) 141–146.
[39] F. Rodríguez-Reinoso, A. Linares-Solano, Chemistry and physics of carbon, Thrower PA, New York, 1988.
[40] R.D. Diehl, T. Seyller, M. Caragiu, G.S. Leathermann, N. Ferralis, K. Pussi, et al., J. Phys. Condens. Matter 16 (2004) 28–39.
[41] M.M. Calbi, M.W. Cole, S.W. Gatica, M.J. Bojan, G. Stan, Rev. Mod. Phys. 73 (2001) 857–860.
[42] C.T. Hsieh, J.M. Chen, R.R. Kuo, Y.H. Huang, Appl. Phys. Lett. 84 (2004) 1186–1190.
[43] N. Sinha, J.Z. Ma, J.T.W. Yeow, J. Nanosci. Nanotechnol. 3 (2006) 573–590.
[44] J.P. Lukaszewicz, Sens. Lett. 4 (2006) 53–98.
[45] T. Pietrass, MRS Bull. 31 (2006) 765–769.
[46] J. Brunet, M. Dubois, A. Pauly, L. Spinelle, A. Ndiaye, K. Guérin, C. Varenne, B. Lauron, Sens. Actuators B 173 (2012) 659–667.
[47] A. Pauly, M. Dubois, J. Brunet, L. Spinelle, A. Ndiaye, K. Guérin, C. Varenne, A.S. Vinogradov, A.Yu. Klyushin, Sens. Actuators B 173 (2012) 652–658.
[48] J.M. Simmons, B.M. Nichols, S.E. Baker, M.S. Marcus, O. Castellini, C.S. Lee, R.J. Hamers, M.A. Eriksson, J. Phys. Chem. B 110 (2006) 7113–7118.
[49] J. Brunet, V. Parra Garcia, A. Pauly, C. Varenne, B. Lauron, Sens. Actuators B 134 (2008) 632–639.
[50] J. Brunet, A. Pauly, C. Varenne, B. Lauron, Sens. Actuators B 130 (2008) 908–916.
[51] J. Simon, P. Bassoul, Design of Molecular Materials: Supramolecular Engineering, John Wiley & Sons, Chichester, 2000.